Synthetic lattices, flat bands and localization in Rydberg quantum simulators in the presence of disorder

Maike Ostmann,[1,2] Matteo Marcuzzi,[1,2] Jiří Minář,[1,2] and Igor Lesanovsky[1,2]

[1] *School of Physics and Astronomy, University of Nottingham, Nottingham, NG7 2RD, UK*
[2] *Centre for the Mathematics and Theoretical Physics of Quantum Non-equilibrium Systems, University of Nottingham, Nottingham NG7 2RD, UK*

The most recent manifestation of cold Rydberg atom quantum simulators that employs tailored optical tweezer arrays enables the study of many-body dynamics under so-called facilitation conditions. Facilitation is a constraint which yields a Hilbert space structure that allows the mapping of many-body states onto artificial – or synthetic – lattices. These lattices feature in general one or several flat bands and may support immobile localized states. We focus our discussion on the simple case of a Rydberg ladder for which we analyze in particular the influence of disorder generated by the uncertainty of the atoms positions. The localization properties of this system are characterized through two correlation lengths. Moreover, we discuss the experimental preparation of an immobile localized state, and analyze disorder-induced propagation effects which may be investigated experimentally.

Over the past few decades, advances in the manipulation of cold and ultra-cold atomic gases made them into a suitable candidate for a versatile quantum simulation platform [1, 2]. Indeed, several paradigmatic many-body models have been studied experimentally, including the Luttinger liquid [3], Tonks-Girardeau gas [4], Bose-Hubbard [5, 6], and Fermi-Hubbard [7], permitting to directly observe several predicted phenomena, such as quantum revivals [8], Lieb-Robinson bounds [9], and topological phase transitions [10].

Among many different physical systems apt to act as quantum simulators, ensembles of Rydberg atoms [11–13] stand out for their strong interactions, which are now known to give rise to an intricate phenomenology [14–24]. These systems are currently employed for a variety of tasks, such as quantum information processing [25–27] and the simulation of quantum spin systems [19, 28]. Several among these instances employ the so-called *anti-blockade* (or *facilitation*) mechanism (see e.g., Refs. [29–35]) to actuate a form of local quantum transport.

In quantum systems, it is well-established that transport can be heavily affected by the presence of quenched disorder, a phenomenon known as Anderson localization [36]. In the presence of randomly-distributed impurities in a metal, for example, different paths taken by an electron can interfere destructively, leading to localization: in other words, the electronic eigenfunctions, far from being extended Bloch waves, become locally peaked with exponentially-suppressed tails. In one and two dimensions, this effect is so relevant that for arbitrarily small disorder all wavefunctions are localized and transport is effectively impossible [37, 38]. Since their first prediction, these effects have been experimentally observed in a range of systems, spanning electron gases [39], cold atoms [40–42], thin films [43] and periodically-driven nitrogen molecules [44].

Besides quenched disorder, localized states can also arise in tight-binding models from particular lattice geometries. In these cases, destructive interference leads to the emergence of flat bands. Models with flat bands typically allow the construction of localized eigenstates, and have been experimentally realized with cold atoms [45], photonic lattices [46], and synthetic solid-state structures [47, 48]. When disorder is introduced in such systems, these pre-existing localized states couple to the dispersive, system-spanning ones and start acting like scatterers, inducing a richer phenomenology, such as localization enhancement [49], Anderson transitions in lower-dimensional systems [50], and disorder-induced delocalization [51].

In this paper we show that Rydberg lattice quantum simulators [19, 28, 52] can be in principle crafted to reproduce disorder phenomena in the presence of flat bands. We demonstrate that under facilitation conditions – when the system parameters are set such that Rydberg states can only be excited next to an already existing excitation – the Hilbert space acquires a regular lattice structure featuring flat bands. In this picture, the uncertainty of atomic positions translates into a disordered potential on the newly created synthetic lattice. Scenarios similar to these were previously theoretically hypothesized in [49, 50]. Here we show that they emerge naturally in Rydberg quantum simulators employing optical tweezer arrays. Using a lattice we shall refer to as "Lieb ladder" as an example we report the scaling of the correlation length and discuss the experimental observation of the spreading dynamics of a local flat-band eigenstate under the action of different disorder strengths.

Rydberg facilitation, Hilbert space structure and flat bands— We start by considering a regular [53] lattice of N optical tweezers, each loaded with a single Rydberg atom, and with nearest-neighbor distance R_0. A laser is shone with a frequency detuned by an amount Δ with respect to an atomic transition between the electronic ground state $|\downarrow\rangle$ and a Rydberg level $|\uparrow\rangle$. We work here in natural units $\hbar = 1$. In a simplified picture, the

atoms can be effectively described as two-level systems. Atoms in the Rydberg state $|\uparrow\rangle$ interact, at distance d, via an algebraically-decaying potential $V(d) = C_\alpha/d^\alpha$, with $\alpha = 3$ for dipole-dipole interactions and $\alpha = 6$ for van-der-Waals ones (without loss of generality, we choose $C_\alpha > 0$). Within the rotating wave approximation the Hamiltonian of this system reads

$$\hat{\mathrm{H}} = \Omega \sum_k^N \hat{\sigma}_x^{(k)} + \Delta \sum_k^N \hat{\mathrm{n}}_k + \frac{1}{2} \sum_{\substack{k=1 \\ m\neq k}}^N V(d_{km})\, \hat{\mathrm{n}}_m\, \hat{\mathrm{n}}_k, \tag{1}$$

where Ω is the laser Rabi frequency, k and m are lattice indices, d_{km} denotes the distance between atoms in sites k and m, $\hat{\sigma}_x^{(k)} = |\uparrow_k\rangle\langle\downarrow_k| + |\downarrow_k\rangle\langle\uparrow_k|$ and $\hat{\mathrm{n}}_k = |\uparrow_k\rangle\langle\uparrow_k|$. The facilitation (or anti-blockade) condition is obtained by setting $\Delta = -V(R_0)$, so that an isolated excited atom makes its neighbors resonant with the laser. In the following, we consider $|\Delta| \gg \Omega$, so that non-facilitated atoms are sufficiently off-resonant to neglect their excitation. Furthermore, we set $V(2R_0) \gg \Omega$ as well. Note that, denoting by R_1 the distance between next-nearest neighbors, $R_0 < R_1 \leq 2R_0$. Hence, the second condition implies that an isolated excitation can facilitate the production of another on a neighboring site, but no additional one can then be produced in the neighborhood, as the process is energetically suppressed. For example, in one dimension $\left|\langle\uparrow\uparrow\uparrow|\, \mathrm{e}^{-iHt}\, |\uparrow\uparrow\downarrow\rangle\right|^2 \sim O((\Omega/V(R_1))^2)$. In the following, we neglect these transitions, effectively splitting the Hilbert space into subspaces separated by energy scales $\gg \Omega$. Each subspace comprises a set of quasi-resonant states separated by scales $\sim O(\Omega)$ (see Ref. [54] for more details on this structure). From a simple perspective, this means that a single excitation can at most produce one more in the neighborhood, after which either the former facilitates the de-excitation of the latter, or vice versa. Starting from a state with a single excitation, the relevant Hilbert subspace will consist of all states with either a single excitation or a single pair of excitations on neighboring sites. Hence, as sketched in Fig. 1 for a few planar examples, a lattice structure emerges in the Hilbert space which closely resembles the geometry of the tweezers. It can be visually reproduced following these rules: (i) in the original lattice structure, draw the links joining nearest neighbors; (ii) identify each site with the state having a single excitation on that site. This exhausts all "one-excitation" states in the subspace; (iii) each "pair" state can be straightforwardly associated to the link joining the two excited atoms; hence, place an additional site in the midpoint of each link and associate it with the corresponding "pair" state. The links in this new-found structure now effectively represent pair of states connected by the Hamiltonian, which can be therefore seen as a tight-binding model on a generalised lattice. In the case of a square lattice, the new structure (see Fig. 1) is called *Lieb lattice* and is known to feature a flat band and two dispersive ones which meet with a linear dispersion at the edges of the first Brillouin zone. However, this construction is general and can be extended to any kind of "regular" lattice. Most of these structures will support flat bands as well: It can be shown [55] that, calling n_1 (n_2) the number of one-excitation (pair) states in a unit cell, the number of flat bands n_{flat} must be $\geq |n_1 - n_2|$. For the examples of Fig. 1, the square, triangular and honeycomb lattices have $(n_1, n_2, n_{\mathrm{flat}}) = (1, 2, 1)$, $(1, 3, 2)$ and $(2, 3, 1)$ respectively. These flat bands constitute extensively-degenerate eigenspaces of the Hamiltonian; as such, it is often possible to recombine the usual (plane-wave-like) Bloch solutions to form a set of localised eigenstates.

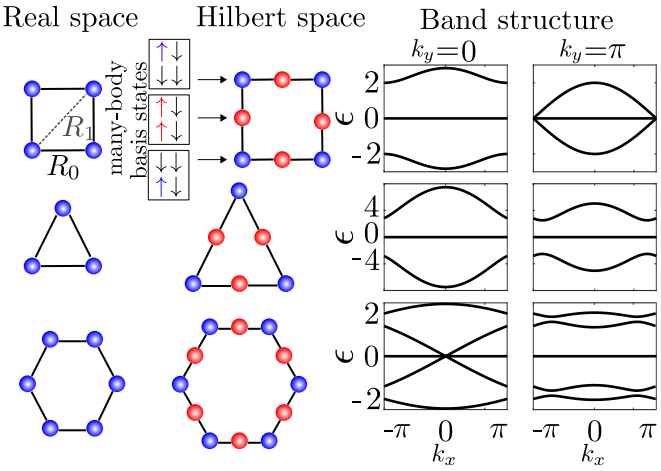

FIG. 1. Left column: geometry of a square, a triangular, and a hexagonal lattice in real space. The blue dots depict the position of the Rydberg atoms and the lines the interaction between neighboring atoms. Middle column: respective "synthetic lattices" in the Hilbert space under the facilitation conditions. The blue dots represent the main state with a single excitation while the red spheres are intermediate state corresponding to a single pair of neighboring excitation. Right column: two cuts of the band structure for each lattice geometries at $k_y = 0$ (left) and $k_y = \pi$ (right). Each lattice features (at least) a flat band. **(We are using k for the lattice indices. Should we change it? Also, the quasi-momentum is expressed in units of $1/R_0$ for the first two cases and in units of $1/R_1$ for the last one.)**

Disorder— Disorder enters the picture through the uncertainty in the atomic positions within the traps. Considering the strength of the interaction potential $V(d)$, even small displacements from the centre of the traps can significantly shift the atomic transitions off resonance from the laser frequency, thereby hindering the facilitation mechanism, as studied e.g. in Ref. [54]. In fact, the interaction potential seen by an atom at a distance $R = R_0 + \delta R$ from an excitation will be $V(R) = V(R_0 + \delta R) \equiv V(R_0) + \delta V$; note that, since $V(R) > 0$, $\delta V > -V(R_0)$, i.e. the energy shifts are only defined on

a domain $[-V(R_0), +\infty)$. At small disorder ($\delta R \ll R_0$) they can be approximated by $\delta V \approx -\alpha C_\alpha / R_0^{\alpha+1} \delta R$. These energy shifts are random and only affect pair states, creating a disordered potential landscape over the pair (red) sites in Fig. 1. The single-excitation (blue) sites' energy remains unvaried instead. We remark here that the Hilbert space structure holds under the introduction of disorder only until the latter is weak, i.e., typically $\delta V \ll V(2R_0)$.

In order to characterize the disorder, we denote by ω the optical trapping frequency (assumed hereafter to be isotropic in space), by m the atomic mass and by T the temperature. The probability distribution of a trapped atom can then be approximately described as a Gaussian of width σ around the trap centre. We require now that (I) $k_B T \gg \hbar\omega$: this implies that one can use the semi-classical estimate $\sigma \approx \sqrt{k_B T / m\omega^2}$ and moreover that the thermal de Broglie wavelength of the atom is much smaller than the distribution width. In other words, the atom can be approximately considered localized somewhere within the trap according to a classical probability distribution. (II) $\omega \Delta t \ll 1$, with Δt the duration of an experiment: this ensures that the atoms will not appreciably move from their positions in this time frame and thus the disorder is quenched. (III) $\Omega \gg \omega$, or in other words the dynamics of the internal degrees of freedom is much faster than the one of the kinetic ones, so that within an experiment one can probe the action of the disordered Hamiltonian on the system while keeping the disorder quenched (i.e. fixed). The properties of the probability distribution of energy shifts are discussed in [55]; here we just remark that amplitudes of shifts over different pair sites are not independent, but correlated **(I still maintain that this comment can be removed, as nothing coming later picks up on it)**.

Disordered Lieb ladder— In the remainder of our discussion, we shall focus on a ladder configuration, i.e. a quasi-one-dimensional lattice formed by placing two linear chains parallel to each other at a lattice spacing distance R_0. For this example, the artificial lattice (corresponding to the "1D Lieb lattice" case of Ref. [49]) in the Hilbert space is sketched in Fig. 2(a). The unit cell consists of five sites with $n_1 = 2$ and $n_2 = 3$ and the band structure features one zero-energy flat and four dispersive bands [Fig. 2 (d)].

This Lieb ladder constitutes one of the simplest examples where flat bands produce a non-trivial interplay with the on-site disorder [49]. In a Rydberg quantum simulator, however, the underlying structure is made more complex **(or simpler?)** by the fact that disorder only appears on pair states. In other words, all the blue sites in Fig. 1(a) are, by construction, unaffected by it. To check how this may affect the spectral properties of the system we study in the following the scaling behaviour of the *localization length* ξ at small disorder and relate, whenever possible, our results to those of Ref. [49], where

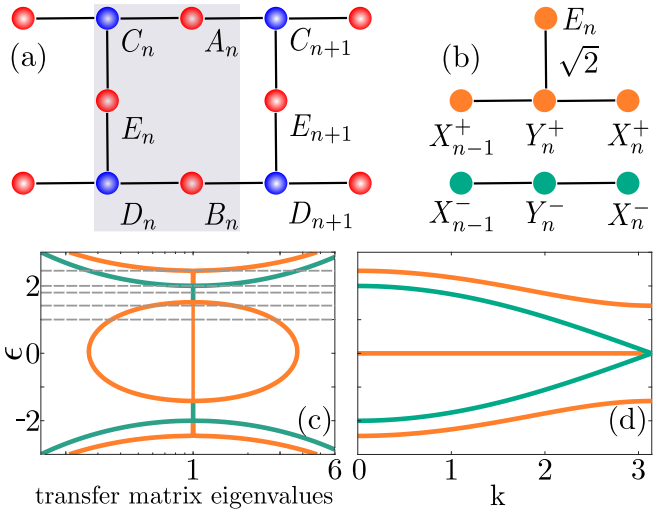

FIG. 2. Hilbert space structure and spectrum in the absence of disorder. (a) One dimensional Lieb ladder. Blue spheres correspond to one-excitation states while red spheres represent pair states. We introduce a convenient notation for the five sites A_n, B_n, C_n, D_n, E_n in the n-th unit cell (shaded grey). (b) A change of basis – the so-called "detangling", introducing the new linear combinations $X_n^\pm$ and $Y_n^\pm$ [49, 56] – maps the Lieb ladder onto two decoupled chains. The $\sqrt{2}$ factor denotes that the hopping amplitude on the vertical link of each unit cell is amplified by that same amount. (c) Eigenvalues of the transfer matrix in log-linear scale. The dotted lines corresponds to the energies $\epsilon = \{0, 1, \sqrt{2}, 1.8, 2, \sqrt{6}\}$ at which the scaling of the localization lengths is investigated in Fig. 3. (d) Band structure of the Lieb ladder. The bands corresponding to the stub lattice are given in red and bands of the ordinary 1D chain are shown in green.

the same geometry is treated with independent disorder on all sites. ξ describes, at fixed energy ϵ, the exponential envelope of eigenstates of the disordered Hamiltonian; in other words, wave functions are peaked and mostly concentrated in a specific area of the lattice and decay as $e^{-x/\xi}$ with the distance r from it (in the longitudinal direction). Via an appropriate change of basis ("detangling transformation" [49, 56]) this Lieb ladder can be mapped onto two uncoupled one-dimensional lattices [see Fig. 2(b)], a chain (in green, supporting the two innermost dispersive bands) and a stub lattice (in red, supporting the flat and two outermost dispersive bands) [55]. For every value of the energy, there are therefore two relevant localization lengths, denoted by $\xi_{1/2}$ with $\xi_1 < \xi_2$, which can be associated to the localization properties of either of the detangled chains of Fig. 2(b). The values $\xi_{1/2}$ are found numerically via a transfer matrix formalism and are displayed in Fig. 3(a) as a function of $s \equiv \sigma / R_0$ and the energy ϵ. In Fig. 3(b) we instead display log-log plots of the correlation lengths at selected energies as functions of s. This highlights the emergence of algebraic scaling $\xi_i \sim s^\nu$. The usual scaling for Anderson localization corresponds to $\nu = 0$ at energies outside

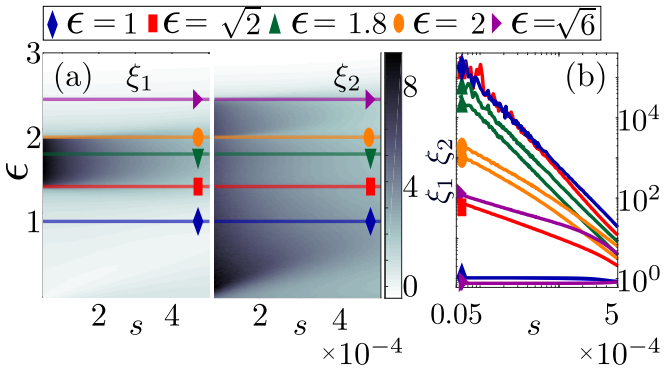

FIG. 3. (a) Localization lengths ξ_1, ξ_2 (color code) as a function of the energy ϵ and the disorder strength $s \equiv \sigma/R_0$. The localization lengths along each of the solid lines are shown in log-log scale in panel (b). For small disorder all lines are approximately linear which allows to assign approximate power law exponents ν characterizing the small-disorder behavior $\xi_i \sim s^\nu$: grouping them by energy ϵ, they read $\nu(\epsilon = 1) \approx \{0.1,\ 2.0\}$, $\nu\left(\epsilon = \sqrt{2}\right) \approx \{0.8,\ 2.2\}$, $\nu(\epsilon = 1.8) \approx \{2.0,\ 2.0\}$, $\nu(\epsilon = 2) \approx \{1.4,\ 1.4\}$, $\nu\left(\epsilon = \sqrt{6}\right) \approx \{0.0,\ 0.8\}$. For these computations, the atomic position distribution is a Gaussian with width σ **[CHECK]**, and the interatomic interaction is a dipole-dipole interaction ($\alpha = 3$) with an interaction strength of $V_0 = 300\Omega$.

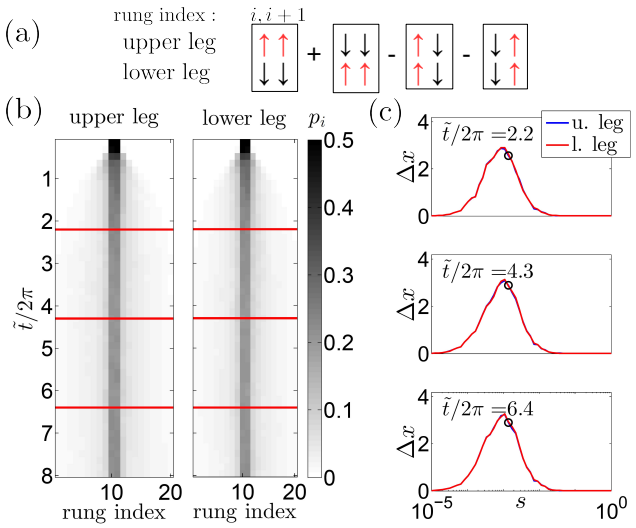

FIG. 4. (a) Schematic representation of the spin configuration corresponding to the initial state $|\psi_{\rm loc}\rangle$ localized at rungs $i, i+1$ of the ladder. (b) The probability of excitations p_i given by the time evolution of the localized state with an initial support in the middle (rungs 10 and 11) of the ladder of length 20 for $s = 0.0014$. The left (right) pane shows the time evolution in the upper (lower) leg of the ladder. The horizontal red lines denote three different times for which the respective value of Δx is shown as a black circle in (c). (c) Standard deviation of the excitation positions Δx vs. the disorder strength s for three different times. Blue (red) solid lines, which are virtually indistinguishable correspond to upper (lower) leg of the ladder respectively. Results obtained for 100 disorder realizations and $V_0 = 200\Omega$.

a band ("out"), $\nu = 2/3$ at a band edge ("edge") and $\nu = 2$ inside a band ("in"). The energies selected in Fig. 2(b) correspond to $\epsilon = 1$ (out/in), $\sqrt{2}$ (edge, in), 1.8 (in/in), 2 (edge/in) and $\sqrt{6}$ (out/edge). In addition, an "anomalous" scaling $\nu = 4/3$ has been found in Ref. [49] at $\epsilon = \sqrt{2}$ and $\sqrt{6}$. This has been attributed to the fact that disorder, in the detangled picture, is not merely on-site but couples the two chains; this in turn may produce resonances between states in the middle of a band and states at the edge of the other one when the latter displays vanishing group velocity. Comparing these values with the ones we have found, we observe reasonable agreement at $\epsilon = 1$ and $\epsilon = 1.8$, for the anomalous scaling at $\epsilon = 2$ and for the "out" scaling at $\epsilon = \sqrt{6}$. The anomalous scaling at $\epsilon = \sqrt{2}$ seems instead to be "cured" as we retrieve a result compatible with the usual Anderson one ($\nu \approx 2$). This is probably due to the "alternating" structure of the disorder in the synthetic lattice, which in the detangled picture results in the absence of random couplings between $Y_n^\pm$ sites, present instead in [49]. **(Should we discuss this in the supplemental? Also, I vote to bring back the table. As it is, this paragraph is almost unreadable and the comparison extremely cryptic.)** It is unclear whether the discrepancies between the "edge" values 0.8 found at $\epsilon = \sqrt{2}$ and $\sqrt{6}$ and the expected 2/3 are simply due to numerical precision, although it seems likely. We have instead no current viable explanation for the 1.4 value found instead of 2/3 at $\epsilon = 2$ and a more detailed investigation may be necessary.

Localized state dynamics— Experimentally measuring the localization lengths studied above is challenging due to the required large systems size and very small noise amplitudes. However, one can probe the influence of disorder by initializing the system in a specific state and tracking the subsequent dynamics by measuring the on-site excitation probabilities [19, 28, 52]. In our case, a particularly interesting choice for an initial state is given by one of the flat band localised states, as it would not spread out if disorder were absent. We prove in [55] that such states take the form $|\psi_{\rm loc}\rangle = 1/\sqrt{4}\left(|A_i\rangle + |B_i\rangle - |E_i\rangle - |E_{i+1}\rangle\right)$ and are entirely localized at rungs $i, i+1$ of the ladder [see Fig. 4(a)]. States of this form can be prepared experimentally via single site addressing (for the protocol see [55]).

The time evolution of the excitation density, when starting from this state is shown in Fig. 4(b). The effect of the disorder becomes apparent in the spreading of the density wave packet which we characterize by the quantity Δx **(not defined at the moment)**. At a given disorder strength s the dynamics reaches quickly a stationary state in which Δx remains constant. It is interesting to observe that Fig. 4(c) shows a non-monotonic behavior as a function of s. This can be easily understood as follows: at very small (but finite) s the initial

state (energy $\epsilon \approx 0$) is almost an eigenstate and it therefore only minimally spreads throughout the system; as s is increased, this picture breaks down and the state more and more strongly connects to other ones, allowing transport to larger distances; at the same time, however, the localization lengths at $\epsilon = 0$ decrease. Hence, an interplay ensues: the spreading δx of the state increases with s as long as the localization length remains larger ($\delta x \ll \xi_i$). Once the decrease in the localization scale catches up with the increase of δx, the behavior is dominated by localization and, as expected, decreases with increasing disorder strength.

Conclusions and Outlook—

Acknowledgments— The research leading to these results has received funding from the European Research Council under the European Unions Seventh Framework Programme (FP/2007-2013)/ERC Grant Agreement No. 335266 (ESCQUMA), the EPSRC Grant No. EP/M014266/1, and the H2020-FETPROACT-2014 Grant No. 640378 (RYSQ). I.L. gratefully acknowledges funding through the Royal Society Wolfson Research Merit Award.

[1] I. Bloch, J. Dalibard, and W. Zwerger, Rev. Mod. Phys. **80**, 885 (2008).
[2] I. Bloch, J. Dalibard, and S. Nascimbene, Nat. Phys. **8**, 267 (2012).
[3] S. Hofferberth, I. Lesanovsky, T. Schumm, A. Imambekov, V. Gritsev, E. Demler, and J. Schmiedmayer, arXiv preprint arXiv:0710.1575 (2007).
[4] T. Kinoshita, T. Wenger, and D. S. Weiss, Science **305**, 1125 (2004).
[5] M. Greiner, O. Mandel, T. Esslinger, T. W. Hänsch, and I. Bloch, nature **415**, 39 (2002).
[6] M. Greiner, O. Mandel, T. Rom, A. Altmeyer, A. Widera, T. Hänsch, and I. Bloch, Physica B: Condensed Matter **329**, 11 (2003).
[7] M. Köhl, H. Moritz, T. Stöferle, K. Günter, and T. Esslinger, Phys. Rev. Lett. **94**, 080403 (2005).
[8] M. Greiner, O. Mandel, T. W. Hänsch, and I. Bloch, Nature **419**, 51 (2002).
[9] M. Cheneau, P. Barmettler, D. Poletti, M. Endres, P. Schauß, T. Fukuhara, C. Gross, I. Bloch, C. Kollath, and S. Kuhr, Nature **481**, 484 (2012).
[10] Z. Hadzibabic, P. Krüger, M. Cheneau, B. Battelier, and J. Dalibard, Nature **441**, 1118 (2006).
[11] M. Saffman, T. Walker, and K. M. lmer, Rev. Mod. Phys. **82**, 2313 (2010).
[12] R. Löw, H. Weimer, J. Nipper, J. B. Balewski, B. Butscher, H. P. Büchler, and T. Pfau, J. Phys. B **45**, 113001 (2012).
[13] T. F. Gallagher, ed., *Rydberg atoms* (Cambridge University Press, Cambridge, 1994).
[14] H. Weimer and H. P. Büchler, Phys. Rev. Lett. **105**, 230403 (2010).
[15] Z. Lan, W. Li, and I. Lesanovsky, Phys. Rev. A **94**, 051603 (2016).
[16] E. Levi, J. Minář, and I. Lesanovsky, Journal of Statistical Mechanics: Theory and Experiment **2016**, 033111 (2016).
[17] Z. Lan, J. Minář, E. Levi, W. Li, and I. Lesanovsky, Phys. Rev. Lett. **115**, 203001 (2015).
[18] H. Schempp, G. Günter, M. Robert-de Saint-Vincent, C. S. Hofmann, D. Breyel, A. Komnik, D. W. Schönleber, M. Gärttner, J. Evers, S. Whitlock, and M. Weidemüller, Phys. Rev. Lett. **112**, 013002 (2014).
[19] P. Schauß, J. Zeiher, T. Fukuhara, S. Hild, M. Cheneau, T. Macrì, T. Pohl, I. Bloch, and C. Groß, Science **347**, 1455 (2015).
[20] R. Löw, H. Weimer, U. Krohn, R. Heidemann, V. Bendkowsky, B. Butscher, H. P. Büchler, and T. Pfau, Phys. Rev. A **80**, 033422 (2009).
[21] N. Šibalić, C. G. Wade, C. S. Adams, K. J. Weatherill, and T. Pohl, Phys. Rev. A **94**, 011401 (2016).
[22] C. Carr, R. Ritter, C. G. Wade, C. S. Adams, and K. J. Weatherill, Phys. Rev. Lett. **111**, 113901 (2013).
[23] M. Marcuzzi, E. Levi, S. Diehl, J. P. Garrahan, and I. Lesanovsky, Phys. Rev. Lett. **113**, 210401 (2014).
[24] R. Gutiérrez, J. P. Garrahan, and I. Lesanovsky, Phys. Rev. E **92**, 062144 (2015).
[25] D. Jaksch, J. I. Cirac, P. Zoller, S. L. Rolston, R. Côté, and M. D. Lukin, Phys. Rev. Lett. **85**, 2208 (2000).
[26] H. Weimer, M. Müller, I. Lesanovsky, P. Zoller, and H. P. Büchler, Nat. Phys. **6**, 382 (2010).
[27] M. Saffman, J. Phys. B **49**, 202001 (2016).
[28] H. Labuhn, D. Barredo, S. Ravets, S. de Léséleuc, T. Macrì, T. Lahaye, and A. Browaeys, Nature **534**, 667 (2016).
[29] C. Ates, T. Pohl, T. Pattard, and J. M. Rost, Phys. Rev. Lett. **98**, 023002 (2007).
[30] T. Amthor, C. Giese, C. S. Hofmann, and M. Weidemüller, Phys. Rev. Lett. **104**, 013001 (2010).
[31] M. Gärttner, K. P. Heeg, T. Gasenzer, and J. Evers, Phys. Rev. A **88**, 043410 (2013).
[32] D. W. Schönleber, M. Gärttner, and J. Evers, Phys. Rev. A **89**, 033421 (2014).
[33] I. Lesanovsky and J. P. Garrahan, Phys. Rev. A **90**, 011603 (2014).
[34] A. Urvoy, F. Ripka, I. Lesanovsky, D. Booth, J. P. Shaffer, T. Pfau, and R. Löw, Phys. Rev. Lett. **114**, 203002 (2015).
[35] M. M. Valado, C. Simonelli, M. D. Hoogerland, I. Lesanovsky, J. P. Garrahan, E. Arimondo, D. Ciampini, and O. Morsch, Phys. Rev. A **93**, 040701 (2016).
[36] P. W. Anderson, Phys. Rev. **109**, 1492 (1958).
[37] N. Mott and W. Twose, Advances in Physics **10**, 107 (1961).
[38] K. Ishii, Progress of Theoretical Physics Supplement **53**, 77 (1973).
[39] M. Cutler and N. F. Mott, Physical Review **181**, 1336 (1969).
[40] J. Billy, V. Josse, Z. Zuo, A. Bernard, B. Hambrecht, P. Lugan, D. Clément, L. Sanchez-Palencia, P. Bouyer, and A. Aspect, Nature **453**, 891 (2008).
[41] G. Roati, C. DErrico, L. Fallani, M. Fattori, C. Fort, M. Zaccanti, G. Modugno, M. Modugno, and M. Inguscio, Nature **453**, 895 (2008).
[42] G. Semeghini, M. Landini, P. Castilho, S. Roy, G. Spagnolli, A. Trenkwalder, M. Fattori, M. Inguscio, and G. Modugno, Nature Physics **11**, 554 (2015).

[43] J. Liao, Y. Ou, X. Feng, S. Yang, C. Lin, W. Yang, K. Wu, K. He, X. Ma, Q.-K. Xue, and Y. Li, Phys. Rev. Lett. **114**, 216601 (2015).
[44] M. Bitter and V. Milner, Phys. Rev. Lett. **117**, 144104 (2016).
[45] R. Shen, L. B. Shao, B. Wang, and D. Y. Xing, Phys. Rev. B **81**, 041410 (2010).
[46] S. Mukherjee, A. Spracklen, D. Choudhury, N. Goldman, P. Öhberg, E. Andersson, and R. R. Thomson, Phys. Rev. Lett. **114**, 245504 (2015).
[47] M. R. Slot, T. S. Gardenier, P. H. Jacobse, G. C. van Miert, S. N. Kempkes, S. J. Zevenhuizen, C. M. Smith, D. Vanmaekelbergh, and I. Swart, Nature Physics (2017).
[48] R. Drost, T. Ojanen, A. Harju, and P. Liljeroth, Nature Physics (2017).
[49] D. Leykam, J. D. Bodyfelt, A. S. Desyatnikov, and S. Flach, The European Physical Journal B **90**, 1 (2017).
[50] J. D. Bodyfelt, D. Leykam, C. Danieli, X. Yu, and S. Flach, Phys. Rev. Lett. **113**, 236403 (2014).
[51] M. Goda, S. Nishino, and H. Matsuda, Phys. Rev. Lett. **96**, 126401 (2006).
[52] H. Bernien, S. Schwartz, A. Keesling, H. Levine, A. Omran, H. Pichler, S. Choi, A. S. Zibrov, M. Endres, M. Greiner, *et al.*, Nature **551**, 579 (2017).
[53] We use here the term "regular" in a loose sense to denote lattices whose primitive lattice (or, if present, basis) vectors all have the same length.
[54] M. Marcuzzi, M. Jiří, D. Barredo, S. de Léséleuc, H. Labuhn, T. Lahaye, A. Browaeys, E. Levi, and I. Lesanovsky, Phys. Rev. Lett. **118**, 063606 (2017).
[55] see supplementary information, .
[56] S. Flach, D. Leykam, J. D. Dodyfelt, P. Matthies, and A. S. Desyatnikov, EPL **105**, 30001 (2014).